Numerical Investigation of the Effect of Screw Geometry on the Mixing of a Viscous Polymer Melt

C. Wang, M. Bussmann, C. B. Park

Department of Mechanical and Industrial Engineering, University of Toronto, 5 King's College Road, Toronto M5S 3G8, Ontario, Canada

Received 19 December 2008; accepted 23 June 2009
DOI 10.1002/app.31039
Published online 26 March 2010 in Wiley InterScience (www.interscience.wiley.com).

ABSTRACT: In polymer extrusion processing, mixing enhancement is an important consideration when an extruder screw is being designed. There are a variety of mixing elements used in the extrusion industry, with little consensus about what differentiates a good mixing section from a poor one. However, good mixing is important for homogenizing the material structure and temperature profile in the flow channel. This article presents a numerical analysis of the role of screw geometry in mixing in a cooling extruder. Four geometries, typical of those used by the extrusion industry, are assessed by the study of the polymer melt flow and heat transfer in the screw channels. © 2010 Wiley Periodicals, Inc. J Appl Polym Sci 117: 775–784, 2010

Key words: computer modeling; extrusion; mixing

INTRODUCTION

In industrial processes, mixing is a unit operation for homogenizing an initially heterogeneous physical system.[1] For example, Figure 1 illustrates a tandem extrusion system used to produce quality microcellular polymer foam. Solid plastic pellets are continuously fed into the first extruder, which melts the polymer, and a foaming gas is then injected into the melt. The second extruder cools and homogenizes the polymer melt to produce a high-volume quality product that feeds an extrusion die. The geometry of the screw in the second extruder plays an important role in mixing, and unlike the screw in the primary extruder, the screw in the secondary extruder is usually not tapered, so the secondary extruder has a constant channel depth. As the use of tandem extrusion lines for producing microcellular foams expands, there is increasing interest in designing better secondary (cooling) screws.

Designing a good cooling screw is challenging because the goal is to simultaneously homogenize the melt and cool it, yet mixing a polymer melt leads to shear reheating because a polymer melt is extremely viscous. The challenge then is to design a screw geometry that mixes without inducing too much shear. To evaluate a screw geometry, one can evaluate the flow patterns within a screw channel, and because a polymer melt has very low thermal conductivity, the heat transfer is largely governed by the flow field, so mixing can also be evaluated by the study of the heat transfer. In this article, we apply such a methodology to compare four screw geometries that are commonly used in secondary extruders by modeling the flow and heat transfer as a means of assessing mixing.

Mixing is often described in terms of two mechanisms, which are defined as distributive and dispersive.[2] Distributive mixing depends on the affine deformation of fluid particles and involves stretching, dividing, and reorienting a fluid to eliminate local variations in material composition to produce a more homogeneous mixture. Distributive mixing can be achieved by the design of convoluted flow paths that repeatedly split and reorient the flow. Dispersive mixing, on the other hand, is characterized by the number of times that fluid particles break and coalesce and can be achieved, for example, by the passage of a mixture through small regions, which leads to intense deformation. Dispersive mixing usually requires a flow to locally exceed a critical stress condition to rupture an agglomerate and so break it up into droplets. Therefore, dispersive mixing, much more than distributive mixing, is associated with intense fluid shear, which for a polymer melt flow leads to shear reheating. As a result, a good cooling screw design will encourage distributive mixing and avoid excessive dispersive mixing.

Simulation tools for modeling flow and heat transfer in extrusion screws became available in the 1970s

Correspondence to: M. Bussmann (bussmann@mie.utoronto.ca).

Contract grant sponsors: Ontario Centres of Excellence, Consortium for Cellular and Microcellular Plastics at the University of Toronto.

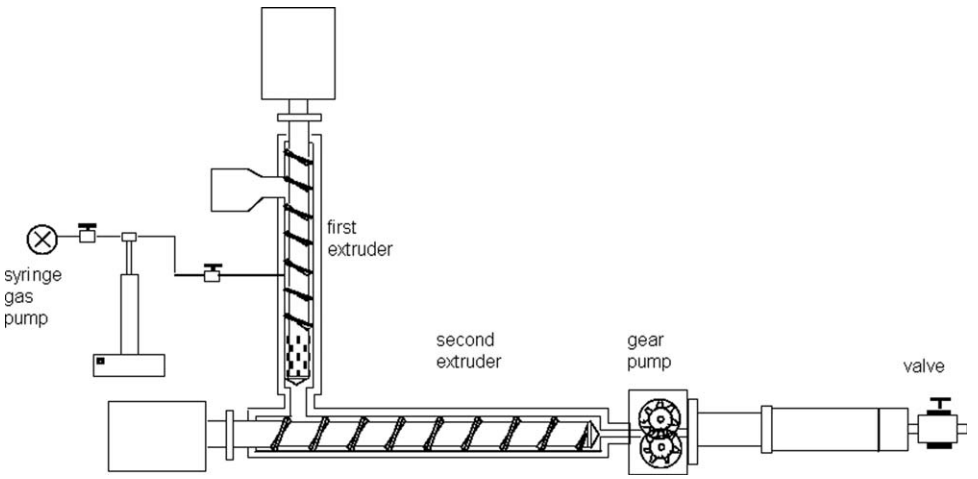

Figure 1 Schematic of a tandem extrusion system.

and allow designers to optimize a design based on mathematical modeling. Much of the early extrusion modeling approximated the melt channel as unwound, and so the flow was assumed to be two-dimensional,[3,4] which is a reasonable approximation for simple screw designs. However, such a methodology cannot be applied to the more complex screws that are available today, and so it has fallen out of favor, being replaced by fully three-dimensional simulations[5,6] that are within the capabilities of modern computer technology.

To quantitatively describe mixing, various approaches have been proposed. Early work was based on the evaluation of the concentration of a minor component in the mixture;[7,8] the dynamics of mixing can also be evaluated by the tracking of the motion of particles in a mixer, and statistical quantities can be used to describe the goodness of a mixture.[9]

Cooling screws, currently in widespread use, have been designed in different ways to improve mixing. One design uses multiflights and small holes in the flights to create extra flow paths,[10] a second design uses segmented multiflights to divide the flow field into smaller regions,[11] and a third design uses different channel depths to further deform the melt.[12] These designs have all been claimed to be superior to a standard screw, but it is not clear to what extent they enhance mixing. Yet understanding the mechanism of mixing in an extruder in response to different geometries is important to guide the direction of future design. This goal can best be achieved by the development of a numerical model based on physical laws and assumptions to predict the melt flow and heat transfer behaviors in response to a given screw geometry.

In the following sections, we describe such a mathematical model, introduce the finite element formulation used to solve the governing equations, and then present results of simulations of the flow and heat transfer of a polypropylene (PP) melt through four screw geometries representative of designs in common use today.

METHODOLOGY

Conservation laws

Polymer melt flow in a cooling extruder is assumed to be steady-state and incompressible and to satisfy the laws of conservation of mass, momentum, and energy, which are in the form of a set of partial differential equations:

$$\nabla \cdot u = 0 \tag{1}$$

$$\frac{\partial u}{\partial t} + u \cdot \nabla u = -\nabla P + \frac{1}{Re} \nabla \cdot \left\{ \frac{\mu(\dot{\gamma})}{\mu_N} \cdot \left[(\nabla u) + (\nabla u)^T \right] \right\} \tag{2}$$

$$\frac{\partial T}{\partial t} + u \cdot \nabla T = \frac{1}{Pe} \left(\nabla^2 T \right) + \Phi \tag{3}$$

where u is the velocity vector, t is time, P is pressure, T is temperature, Φ is the heat dissipation term, $\dot{\gamma}$ is the shear rate, and μ_N is the Newtonian viscosity. The previous equations are in a nondimensional form and contain two nondimensional numbers:

1. The Reynolds number: $Re = \rho UL/\mu$.
2. The Peclet number: $Pe = UL/D$.

where ρ is the fluid density, μ is the dynamic viscosity, L is a flow characteristic length, U is a characteristic velocity, and D is the thermal diffusivity. For a molten polymer flow, Re is always very small ($\ll 1$) because of the high viscosity of the melt, so the flow field is diffusion-dominated. On the other hand, the typical Pe value is large because of the low

thermal diffusivity of the polymer melt; typical values of thermal diffusivity are in the range of 10^{-5} to 10^{-6} m^2/s, and this yields a large P_e value of the order of 10^4. This makes heat transfer advection-dominated. This large P_e value effectively insulates the melt in the interior of the screw channel from the melt near the barrel. Therefore, heat transfer can mainly be enhanced by the variation of flow patterns.

The polymer melt is modeled as a purely viscous fluid. Shear rate $\dot{\gamma}$ and the temperature-dependent viscosity of the melt are described by a modified power-law model:

$$\mu(\dot{\gamma}) = m(\dot{\gamma})^{n-1} e^{-b(T-T_b)} \tag{4}$$

where m is the consistency index ($Pa{\cdot}s^n$), b is a constant, T_b is a reference temperature, and n is the power-law index.

In general, eqs. (2) and (3), for the velocity and temperature fields, are coupled with the viscosity and shear reheating terms, so the equations must be solved simultaneously. However, because we assess mixing primarily by examining the flow field and because (as we will show) we consider the flow and heat transfer within just one turn of a screw, over which the temperature does not vary significantly, we have simplified the numerics by decoupling the flow and heat transfer equations, calculating the flow while assuming an isothermal condition, and then solving the energy equation subsequently. Therefore, only a $\dot{\gamma}$-dependent viscosity model, $\mu(\dot{\gamma}) = m(\dot{\gamma})^{n-1}$, was used for the modeling.

Numerical algorithm

Finite element solvers for three-dimensional non-Newtonian fluid flow and advection–diffusion heat transfer have been developed on the basis of two existing finite element solvers.[13,14] The governing equations [eqs. (1)–(3)] are spatially discretized with a Galerkin finite element approach in conjunction with tetrahedral elements that have 10 nodes for velocity and temperature and 4 nodes for pressure. The unknown velocity, pressure, and temperature fields are expressed in terms of the shape functions ϕ_j and ψ_j and the nodal velocity, pressure, and temperature values (u_j, p_j, and T_j, respectively):

$$u = \sum_{j=1}^{N} u_j \phi_j \tag{5}$$

$$T = \sum_{j=1}^{N} T_j \phi_j \tag{6}$$

$$p = \sum_{j=1}^{N_p} p_j \psi_j \tag{7}$$

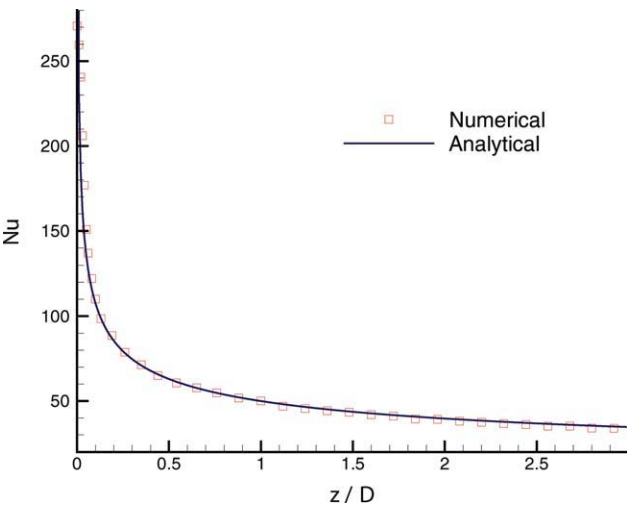

Figure 2 Nusselt number (Nu) vs axial position (z/D) along the inner barrel surface. [Color figure can be viewed in the online issue, which is available at www.interscience.wiley.com.]

where there are $N = 10$ degrees of freedom for velocity (in each coordinate direction) and temperature and $N_p = 4$ degrees of freedom for pressure. Following a Galerkin spatial discretization, we can write the governing equations in a semidiscrete form as follows:

$$[\mathrm{M}]\frac{d\{\mathrm{u}\}}{dt} + [\mathrm{S}]\{\mathrm{u}\} + [\mathrm{L}]^T\{\mathrm{p}\} = \int_{\Gamma} \left(-p\mathrm{n} + \frac{\partial u}{\partial \mathrm{n}}\right) d\Gamma \tag{8}$$

$$[\mathrm{L}]\{\mathrm{u}\} = 0 \tag{9}$$

$$\frac{\partial\{\mathrm{T}\}}{\partial t} = D\{\mathrm{T}\} + C\{\mathrm{T}\} + f \tag{10}$$

where {u}, {p}, and {T} are the vectors of the nodal velocity, temperature, and pressure, respectively; [M], [S], and [L] are elemental matrices; $D = \nabla^2 T/Pe$ is the diffusion operator; $C = -u\nabla$ is the advection operator; Γ is the boundary of the elemental volume; f is the heat dissipation term; and n is a normal vector.

The non-Newtonian flow solver was validated by the calculation of the steady flow of a power-law fluid in a straight pipe, and it showed excellent agreement with the analytical solution and experimental data. The advection–diffusion heat transfer solver was validated with the Graetz-Nusselt problem,[15] which describes the development of a heat transfer boundary layer in a fully developed laminar flow in a cylindrical tube; a comparison of the numerical and analytical results is presented in Figure 2.

Boundary conditions

A cooling screw is usually designed with one or multiple helical threads twisted along a cylinder,

and the flow channel is between the screw and the surrounding barrel. The screw rotates within a stationary barrel, and so a nonslip boundary condition was applied everywhere along the screw, with the velocity of each node calculated from the screw revolution speed, as illustrated in Figure 3.

Because the flow geometry is a periodic flow channel with a large length-to-diameter ratio, a periodic inflow/outflow boundary condition was implemented to simulate fully developed flow in a way that conserves the initially specified volumetric flow rate. For the heat transfer modeling, the barrel temperature was specified, as was the temperature of the melt entering the screw element, and a zero heat flux was assumed at the screw root.

Mixing evaluation

To quantitatively describe mixing, recent developments in the field of dynamic systems have led to an approach to understanding the kinematics of fluid mixing. A mathematical framework for the analysis of mixing systems, simultaneously considering the shear strain and the orientation of fluid elements, has been advanced by Ottino[16] and has shown how local stretching rates can be used to quantify dispersive mixing by the use of the local mixing efficiency (e):

$$e = \left| \frac{\mathrm{D} : nn}{\sqrt{\mathrm{D} : \mathrm{D}}} \right| \tag{11}$$

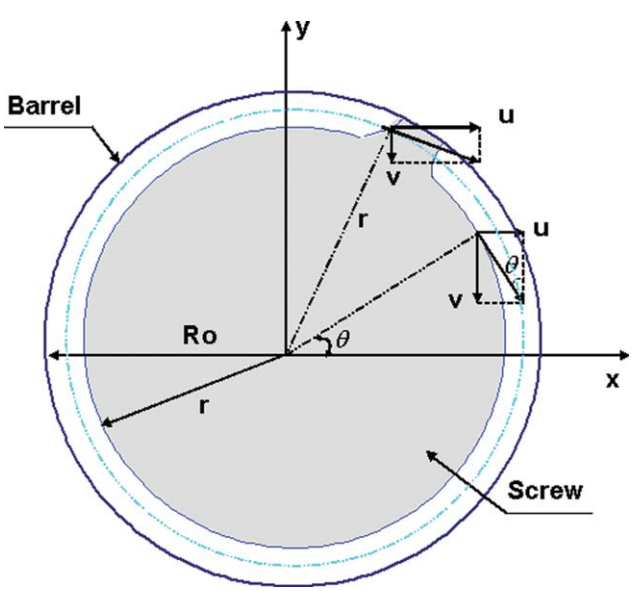

Figure 3 Velocity boundary conditions along the screw (barrel velocity = 0); Ro is the barrel radius, r is the radius of an arbitrary point on the screw, u is the velocity in the x direction, and v is the velocity in the y direction. [Color figure can be viewed in the online issue, which is available at www.interscience. wiley.com.]

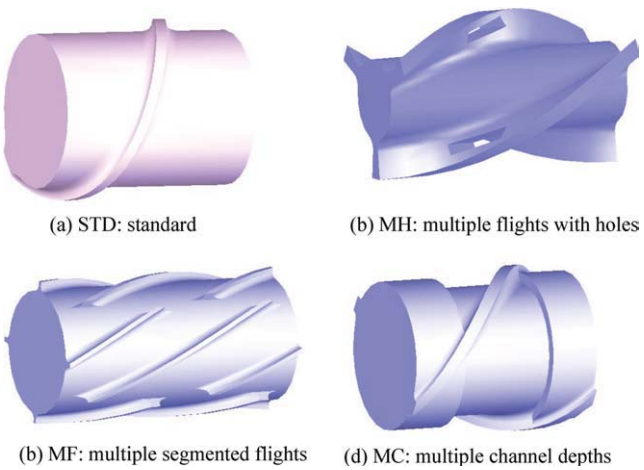

Figure 4 Screw elements. [Color figure can be viewed in the online issue, which is available at www.interscience. wiley.com.]

where n is the normal direction of the interfacial area, which can be defined as $n_i = u_i / \sqrt{u_j u_j}$; D is the rate of deformation tensor; and $\mathrm{D} : \mathrm{D} = \sum_i \sum_j \mathrm{D}_{ij}\mathrm{D}_{ji}$.

Another measure of mixing is the so-called average residence or dwell time of a fluid element within an extruder ($\bar{t}$), which is equivalent to the rate at which a polymer melt moves through an extruder in a steady state and is equal to the total channel volume (V) divided by the volumetric flow rate (Q):

$$\bar{t} = V/Q \tag{12}$$

Mixing and cooling typically benefit from a longer average residence time.

RESULTS AND DISCUSSION

Screw geometries

An STD (standard) screw geometry [Fig. 4(a)] and three specially designed screws [Fig. 4(b–d)] have been studied. Figure 4(b) shows a multiflight screw with holes through the flights (MH); Figure 4(c) shows a screw with segmented multiflights (MS). Figure 4(d) shows a multiflight screw with two different channel depths (MC). A summary of the geometrical information for all four screw elements is listed in Table I.

These geometries were spatially discretized with the commercial software ICEMS-CFD[17] and then studied by numerical modeling of the flow and heat transfer in the screw channels. The finite element mesh for the standard cooling screw channel is shown in Figure 5(a); it contains 692,058 tetrahedral elements and 1,121,725 nodes. Progressively refined meshes for one pitch length of the screw channel were constructed to ensure that the simulation results were mesh-independent. Similarly, Figure

TABLE I
Geometrical Dimensions of the Screw Elements

Dimension	Screw element			
	Standard screw	MH screw	MS screw	MC screw
Number of flights	1	3	4	2
Barrel diameter (in.)	0.75	0.75	0.75	0.75
Axial screw length (in.)	1.65	2.54	3.13	1.977
Screw channel height (in.)	0.1	0.4	0.1	0.1/0.2[a]

[a] The MC screw had two channel depths.

5(b–d) illustrates the finite element meshes for the other screw elements.

The material considered in this study is WB130HMS PP, which we consider representative of polymers used for extrusion processing. The choice of the polymer affects only the constants in the viscosity equation, and the shear-thinning viscosity power-law model is suitable for most polymer melts (e.g., polystyrene, polyethylene, and high-density polyethylene). Moreover, most polymer melts have low thermal diffusivity, which leads to a large P_e value. Therefore, we believe that the modeling and the conclusions that we draw are generally applicable to most of the materials used in polymer extrusion processing. PP was assumed to enter the screw element at an initial temperature of 230°C, whereas the barrel temperature was maintained at 190°C. The screw rotation speed and the polymer melt flow rate were values typical of a laboratory extruder. A summary of the material data used for the calculations and the operating conditions considered are listed in Table II and have been taken from ref. 18.

The R_e and P_e values for each case were calculated with a characteristic velocity, which was based on the average axial fluid velocity, and a characteristic flow length, which was defined as the screw channel depth from the screw root to the barrel. Parameters related to the flow and heat transfer simulations for each case are listed in Table III.

Velocity field

Velocity fields were calculated for PP melt flow in the channel between an outside barrel and each of the four screw elements illustrated in Figure 4. The time to compute the steady flow through one pitch of the screw channel (with periodic inflow/outflow

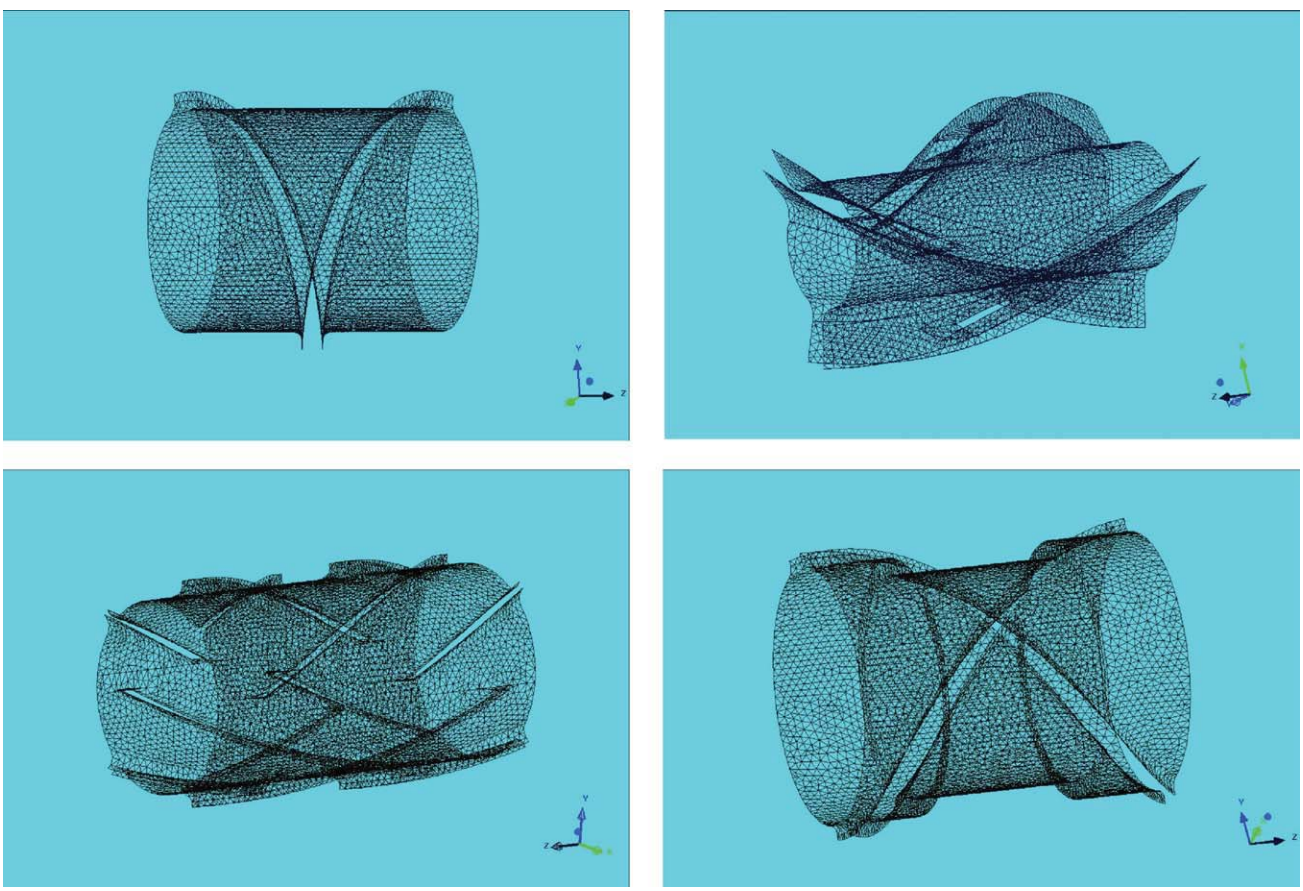

Figure 5 Finite element meshes for the screws depicted in Figure 4. [Color figure can be viewed in the online issue, which is available at www.interscience.wiley.com.]

TABLE II
Material Data and Operating Conditions

Parameter	Quantity
Screw revolution speed (rpm)	8
Mass flow rate (g/min)	20
Barrel temperature (°C)	190
Inflow temperature (°C)	230
Power-law index (n)	0.4
μ_N	6000.0
Thermal diffusivity (m^2/s)	1.2×10^{-7}
Density (g/mL)	0.910

This table was adapted from Wang and Park.[18]

TABLE III
Parameters for Flow and Heat Transfer Modeling

Screw element	Characteristic velocity (m/s)	Characteristic length (m)	*Re*	*Pe*
STD	7.62×10^{-2}	2.45×10^{-4}	2.94×10^{-5}	1.61×10^{3}
MH	2.72×10^{-2}	1.02×10^{-3}	4.19×10^{-5}	2.30×10^{3}
MS	5.97×10^{-2}	3.05×10^{-4}	2.30×10^{-5}	1.26×10^{3}
MC	5.61×10^{-2}	3.81×10^{-4}	5.25×10^{-5}	1.18×10^{3}

conditions applied) was about 20 h on an Intel Pentium 4 computer (2.0-GHz CPU and 2 GB of RAM) running the Linux operating system. Figure 6 illustrates the axial velocity at cross sections of each of these screw channels; the specially designed screw geometries yield small regions of reversed flow, as evidenced by negative axial velocities. Figure 7 illustrates streamlines within the screw channels for all four simulations.

Compared to the more complex screws, the standard cooling screw yields the simplest flow pattern [Figs. 6(a) and 7(a)]. The MH screw, illustrated in Figures 6(b) and 7(b), has a much deeper channel depth, and the three flights split the flow field into three parts. The streamline trace in Figure 7(b) shows that across the channel of the MH screw, vortices form because of the particular configuration of this screw element, and these are indicative of distributive mixing. On the other hand, the holes in the flights, which provide extra flow paths with a high velocity at the center of each of the holes, clearly contribute to dispersive mixing. The MS screw, illustrated in Figures 6(c) and 7(c), with its multiple segmented flights also generates a more complicated flow pattern, as the segmented flights force the melt to flow back and forth axially, and this would contribute to distributive mixing. Finally, the flow field around an MC screw (with two flights and different channel depths) is illustrated in Figures 6(d) and 7(d). The velocity contour plot indicates that the flow patterns in the two channel depths are different

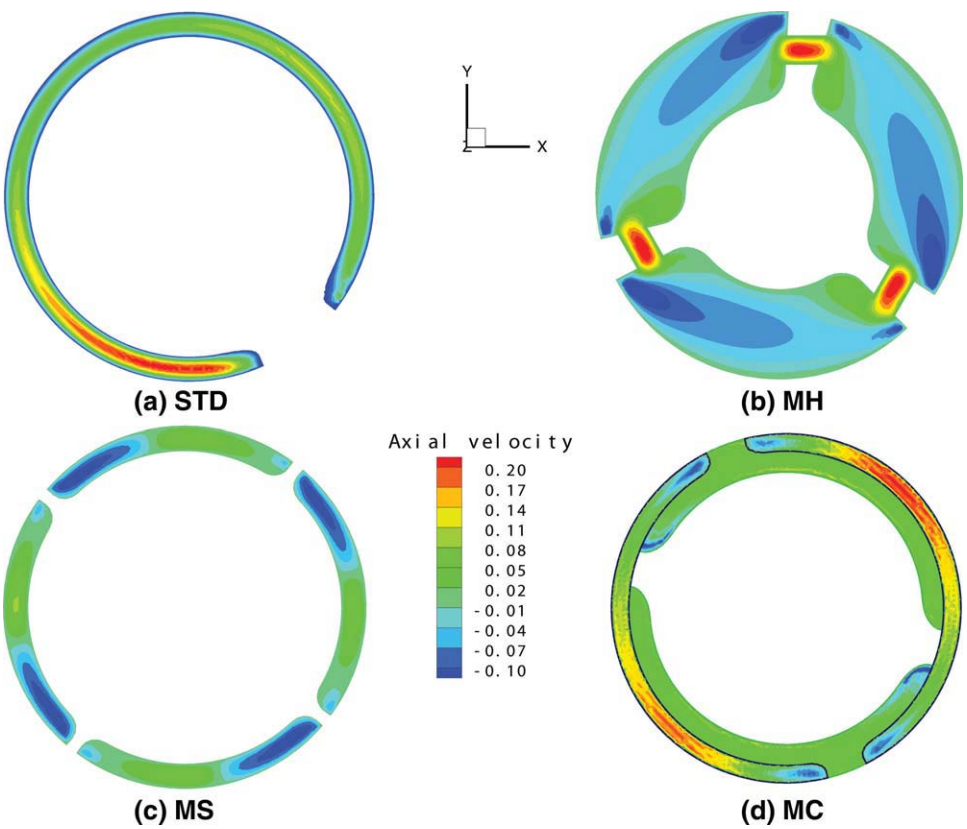

Figure 6 Axial velocity contours. [Color figure can be viewed in the online issue, which is available at www.interscience.wiley.com.]

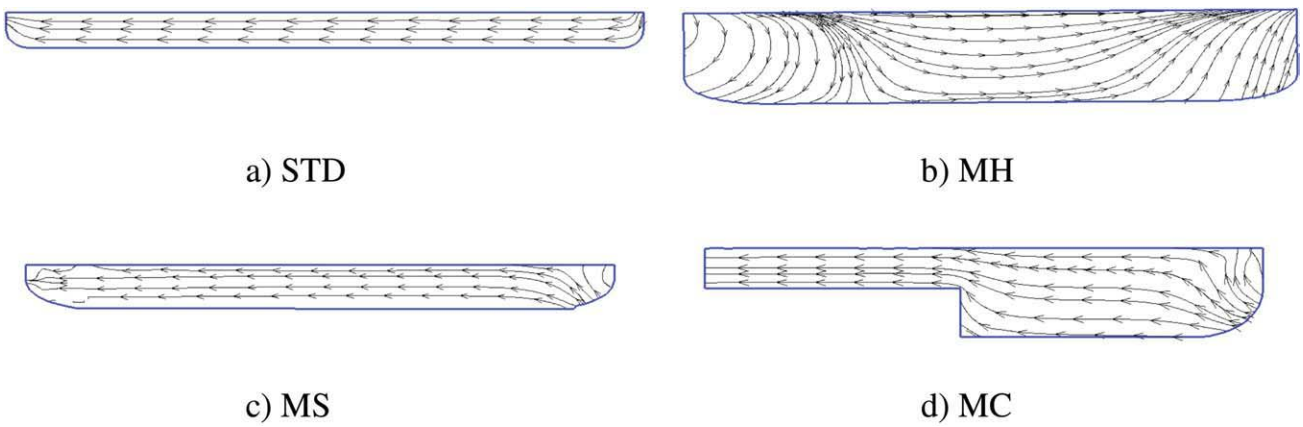

Figure 7 Velocity streamlines within the screw channels.

and that the fluid stretches as the melt crosses from one channel to another; the streamlines indicate that the different channel depths yield a flow field that is intensely stretched while passing through the channel and so provides a significant deformation of the melt flow, albeit one that is likely dispersive and so contributes to shear reheating.

The simulation results clearly indicate that the more complex flow patterns in these specially designed screws are advantageous to mixing, and as a result, we surmise that they are superior to a standard screw.

Pressure field: A comparison with an experimental result

One of the important measures of an extrusion process is throughput. There are usually two components of flow in an extruder: the drag flow and the pressure flow. The drag flow arises from the relative motion of the liquid (due to the rotating screw) and the stationary barrel. The pressure flow arises from the back pressure caused by the buildup of pressure in the extruder during the extrusion process, but it is a negative contribution to flow and so reduces the throughput. The pressure profile for the standard screw geometry is plotted in Figure 8. For the standard screw, the pressure rises along the channel (the jump in pressure midway along the element is due to the presence of the screw flight). We also conducted a simple experiment by installing two pressure transducers at each end of a laboratory second extruder with a standard cooling screw. We then divided the overall difference in measured pressure along the extruder by the number of pitches of the cooling screw to obtain an average pressure variation along one pitch, and we illustrate that difference by plotting two values of pressure in Figure 8. The measured pressure difference is very similar to the calculated one and indicates that for this case, as shown by the operating conditions listed in Table I, the pressure contributes negatively to the overall throughput for the standard screw.

Local mixing efficiency

Figure 9 illustrates the local mixing efficiency, which is indicative of dispersive mixing [see eq. (11)], in the four screw channels. Other than near the flights, the value of the local mixing efficiency in these channels is small, indicating that most of the stress is generated at the tips of the screw flights, which causes fluid particles to break down and so leads to dispersive mixing.

The value of the mixing index for the standard screw is smaller than that for the other screws because mixing is induced only by unidirectional shear flow, which is the least effective mixing mechanism. The MC screw, on the other hand, appears to show the highest value of mixing efficiency, which

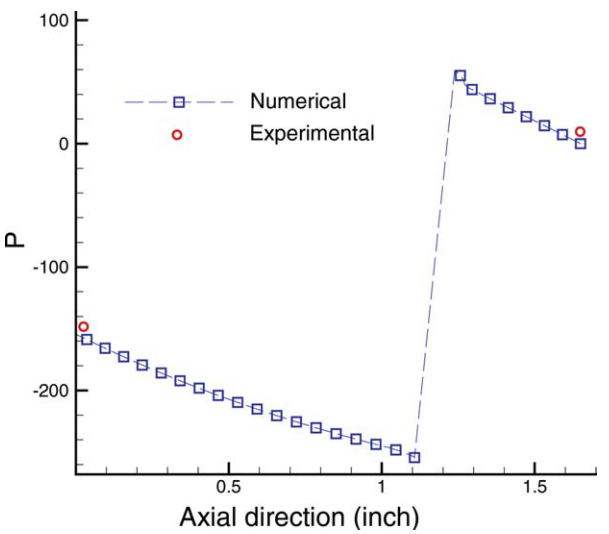

Figure 8 Pressure profile for the standard screw geometry and a comparison with experimental results. [Color figure can be viewed in the online issue, which is available at www.interscience.wiley.com.]

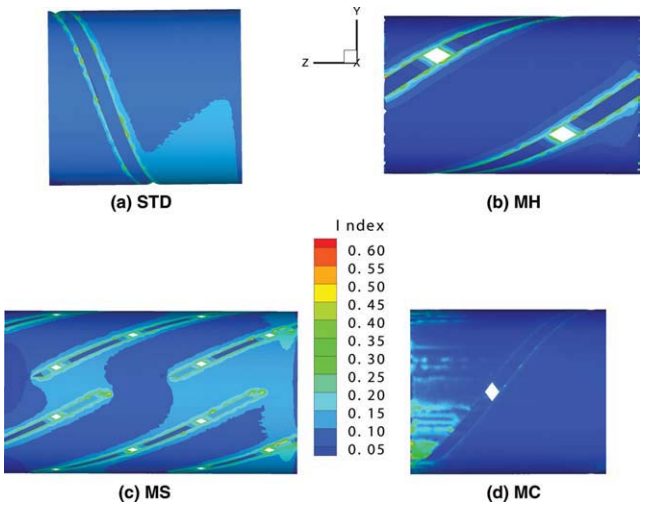

Figure 9 Local mixing index. [Color figure can be viewed in the online issue, which is available at www.interscience.wiley.com.]

implies greater dispersive mixing in this screw channel, which would induce significant shear reheating. This is because the MC screw has different channel depths, and thus fluid particles are stretched more when they pass between the different channels, adding to the deformation of the melt.

Table IV shows the average residence time [eq. (12)] for the four screws at a fixed flow rate. The shortest time is for one turn of the standard screw, about 30 s, whereas the MH screw has the longest residence time because of its deeper channel. Table IV clearly indicates that the melt will remain longer inside the specially designed screw elements, which promote both mixing and cooling.

Heat transfer

Heat transfer in an extruder is limited by the low thermal diffusivity of a polymer melt, which results in a large *Pe* value (recall that $Pe = UL/D$ characterizes the rate of thermal advection with respect to the rate of thermal diffusion). The same material in different flow channels will yield somewhat different *Pe* values. On the other hand, the thermal diffusivity of fluids can vary by orders of magnitude, so within the same screw geometry, *Pe* can vary dramatically. To illustrate the effect of *Pe* on heat transfer, Figure 10 illustrates the temperature profiles along the cross section of a standard screw for *Pe* values of 10, 100, 1000, and 10,000. For the same geometry, this is akin to varying the thermal diffusivity. Given the same flow field, low values of *Pe* (10 and 100) correspond to a fluid that can quickly diffuse heat to the cold barrel. As *Pe* increases (and thermal diffusivity decreases, the heat within the melt (accumulated in the first extruder) is carried along as the melt flows in the cooling extruder [Fig. 10(c,d)]. Only a very thin thermal boundary layer forms, and only a small amount of heat is transmitted to the cooled barrel.

Heat transfer was then calculated for all four screw geometries with the same material. Figure 11(a–d) illustrates the temperature profiles across screw channels for each screw element. Details of the thermal boundary layers and the melt temperature distribution across the flow channel at A–A from the screw root to the barrel are plotted in Figure 12.

For the MH screw [Fig. 11(b)], only about a third of the fluid is affected by the cold barrel; the rest of the fluid maintains the heat that it contained when it entered the channel. The standard screw element and the MS screw element [Fig. 11(a,c)] have similar temperature distributions, and the average temperature is less than that of the MH screw. Figure 11(d) shows that using different channel depths improves

TABLE IV
Average Residence Times

Screw element	Average residence time (s)
STD	31
MH	142
MS	80
MC	68

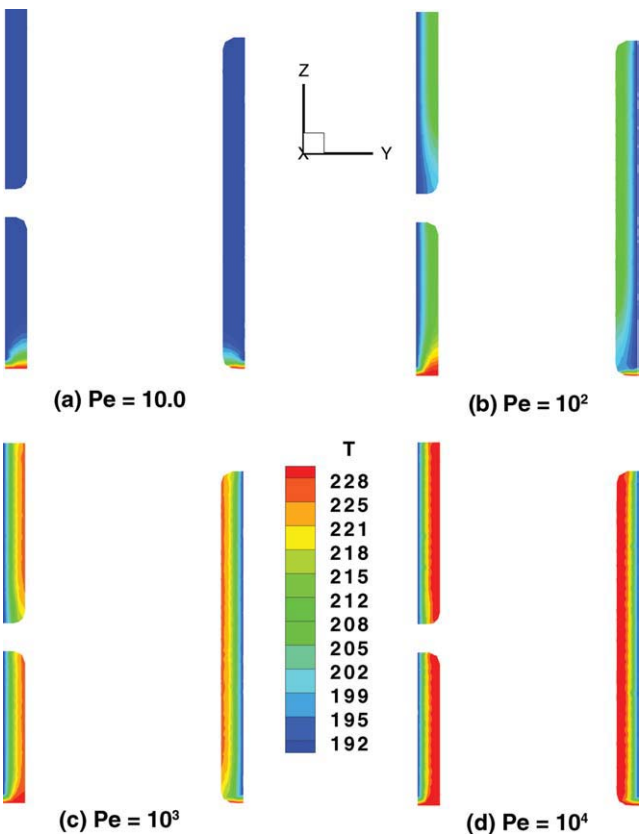

Figure 10 Effect of *Pe* on the heat transfer. [Color figure can be viewed in the online issue, which is available at www.interscience.wiley.com.]

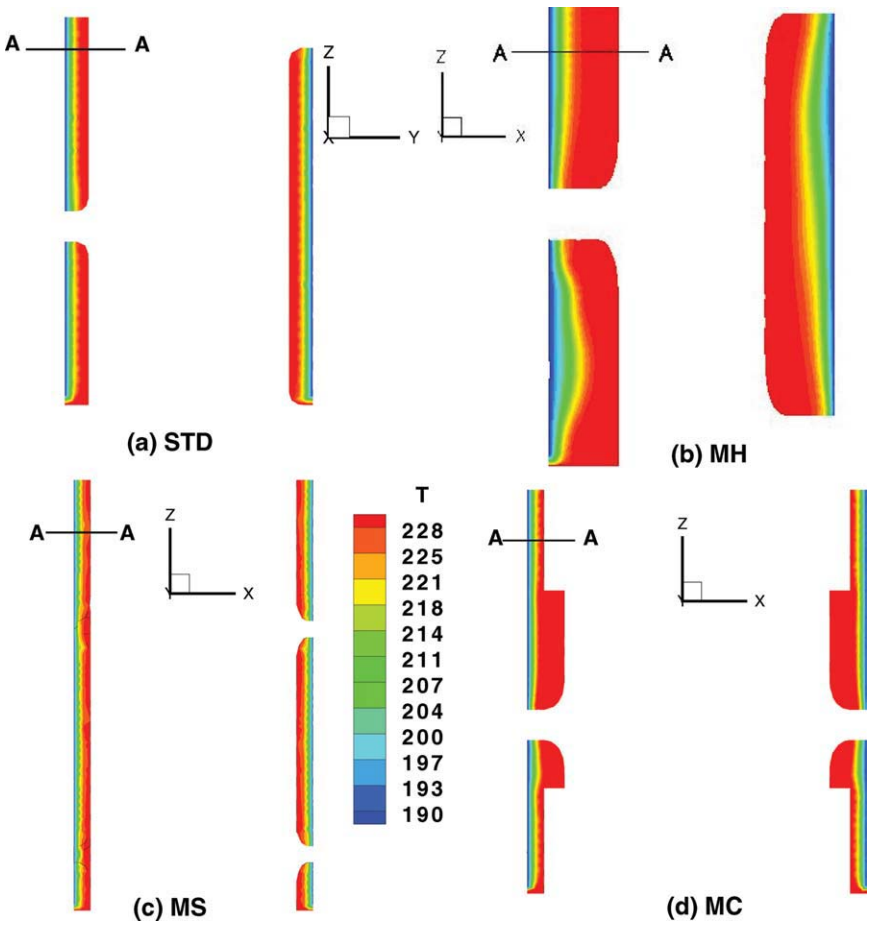

Figure 11 Temperature fields. [Color figure can be viewed in the online issue, which is available at www.interscience.wiley.com.]

heat diffusion in the smaller channel, so the average temperature is lower than that of the other cases. Figure 12 indicates that although the flow fields of these four cases are different, the heat transfer is limited because of the limited heat diffusion between melt particles; therefore, the temperature profiles for these cases are similar, and this implies that mixing improvement does not significantly affect the heat transfer for a high-*Pe* material and that cooling may not be sufficient if only the extruder barrel serves as a cooling device.

CONCLUSIONS

A finite element analysis for solving three-dimensional polymer melt flow and heat transfer in four cooling screws was carried out to investigate the effect of screw geometry on mixing. The flow and heat transfer analyses were decoupled to simplify the calculations, so we did not consider shear reheating. Given that we calculated flow through only one turn of each screw and that mixing was assessed primarily as a function of the flow field, we consider this a reasonable simplification.

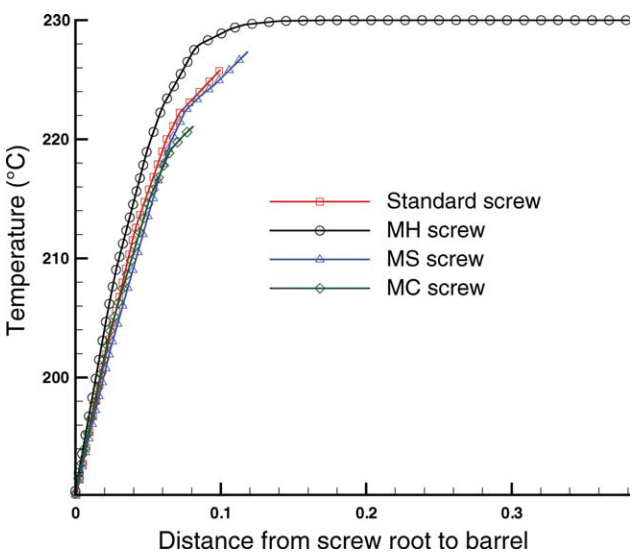

Figure 12 Temperature across the channel at cross sections along A–A (as depicted in Fig. 11). [Color figure can be viewed in the online issue, which is available at www.interscience.wiley.com.]

Polymer melts have a very limited capability to diffuse heat. Therefore, homogeneity in an extruder can be achieved only by the provision of sufficient mixing of the melt particles, which can be obtained by diversification of the flow pattern with special screw geometries. In general, better homogenization is possible with multiflight screws, and diversified flow patterns can be obtained by the use of multiple flights and by the incorporation of elements to provide extra flow paths to divide and reorient the flow (e.g., the MH and MS screws). Compared to the more complex screws, the standard cooling screw provides the least distributive and dispersive mixing. The screw with multiple segmented flights (MS screw) produces good distributive mixing; the multiflight screw with holes through the flights (MH screw) and the screw with two flights and different channel depths (MC screw) contribute to both distributive and dispersive mixing and especially enhance dispersive mixing. However, intense dispersive mixing will induce significant shear reheating, which must be avoided when a screw is being designed.

Although a homogeneous melt distribution can be obtained by the provision of good mixing, cooling is limited if the only heat transfer path is through the barrel. This study provides a tool for the subsequent design of an optimal technical solution for the elements of an extruder.

References

1. Chung, C. I. Extrusion of Polymers: Theory and Practice; Hanser: Cincinnati, OH, 2000.
2. Tadmor, Z.; Gogos, C. Principles of Polymer Processing; Wiley-Interscience: New York, 2006.
3. Syrjala, S. Numer Heat Transfer A 1999, 35, 25.
4. Syrjala, S. Numer Heat Transfer A 2000, 37, 897.
5. Tzoganakis, C.; Karagiannis, A. Polym Eng Sci 1996, 36, 1796.
6. Hwang, W. R.; Kwon, T. H. Polym Eng Sci 2000, 40, 702.
7. Sturman, R.; Ottino, J. M.; Wiggins, S. The Mathematical Foundations of Mixing; Cambridge University Press: Cambridge, England, 2006.
8. Darkwerts, P. V. Appl Sci Res 1952, 3, 279.
9. King, R. Fluid Mechanics of Mixing: Modelling, Operations and Experimental Techniques; Kluwer Academic: Oxford, 1992.
10. Fogarty, J.; Fogarty, J.; Rauwendaal, C. Soc Plast Eng Annu Tech Conf Tech Pap 2001, 298–305.
11. Rauwendaal, C. Plastics, Rubber and Composites 2004, 33, 397–399.
12. Somers, S. A.; Spalding, M. A.; Dooley, J.; Hyun, K. S. Soc Plast Eng Annu Tech Conf Tech Pap 1995, 41, 22.
13. Minev, P.; Ethier, C. Comput Methods Appl Mech Eng 2003, 192, 1281.
14. Mofrad, M.; Ethier, C. Comput Methods Appl Mech Eng 2002, 191, 5345.
15. Cussler, E. Diffusion: Mass Transfer in Fluid Systems; Cambridge University Press: New York, 1997.
16. Ottino, J. M. The Kinematics of Mixing: Stretching, Chaos, and Transport; Cambridge University Press: New York, 1989.
17. ICEM CFD 11.0; ANSYS ICEM CFD Engineering: Worthington, Ohio, 2008.
18. Wang, J.; Park, C. B. Soc Plast Eng Annu Tech Conf Tech Pap 2006, 896–902.